Hindawi
Material Design & Processing Communications
Volume 2023, Article ID 6551830, 17 pages
https://doi.org/10.1155/2023/6551830

Research Article

Experimental Investigations of Damage Identification for Aluminum Foam Sandwich Beams Using Two-Step Method

Xinyu He[1], **Dongsheng Ge**[2] **and Yi An**[3]

[1]*School of Mechanical and Power Engineering, Nanjing Tech University, Jiangsu, Nanjing, China*
[2]*Secondary Specialized School of Nanjing-Pukou, Jiangsu, Nanjing, China*
[3]*School of Physical and Mathematical Sciences, Nanjing Tech University, Jiangsu, Nanjing, China*

Correspondence should be addressed to Yi An; anyi@njtech.edu.cn

Received 27 October 2022; Revised 9 September 2023; Accepted 11 September 2023; Published 22 November 2023

Academic Editor: Guian Qian

In the experiment, strain gauges and dynamic signal acquisition instruments are used to collect and record data, and the stochastic subspace algorithm is used to extract the first three strain modal parameters of each case. The damage amount identified by the second natural frequency based on the modified Timoshenko beam theory is more in line with the actual situation. The damage depth of case 2 and case 4 is 2 mm, and the identified damage amount is 10% and 9%, respectively. The damage depth of case 3 and case 5 is 4 mm, and the identified damage amount is 16% and 23%, respectively. The damage location information of case 6 is well identified by using the normalized strain modal shape difference index and the enhanced strain modal shape difference index. Taking the strain response signal of case 6 as an example, it is proved that the stochastic subspace strain modal parameter identification algorithm has strong anti-interference ability under the action of 1.5 times, 4 times, and 9 times noise. In addition, the method is verified by theoretical calculation and numerical simulation, and the damage law has a high degree of coincidence with the test. The experimental results show that this method expands the theoretical basis of foam metal damage degree information identification and improves the accuracy of damage location information identification and the anti-interference of parameter identification.

1. Introduction

As a lightweight component, aluminum foam sandwich structure is widely used in rail transit, ship transportation, aerospace, and other fields, such as large space station panel, rocket shell, ship side panel, car crossbeam, and door built-in anticollision protection beam [1–5]. In general, internal defects are inevitable when the structure is in service, so the health of the structure should be monitored in time in order to eliminate potential safety hazard.

At present, it is a very hot topic that the damage identification theory is based on structural dynamic characteristics [6–9]. Wahyu et al. [10] identified three types of damage of carbon/epoxy resin laminated composite beam by curvature mode and experiment. Cao et al. [11] used static deflection and modal shapes to detect the damage of the cantilever beam and discussed the sensitivity of the corresponding indexes. Saeed et al. [12] studied the antinoise performance of the new technology which combines curvature mode with gapped smoothing method in damage identification of plate structures. Compared with the strain mode index, the above methods contain numerical calculation errors in the index transformation, and it is difficult to identify damage near modal nodes, and this kind of method needs to establish a damage information database for the identification of damage degree information. According to the way of collecting excitation information or not, the method of modal parameter identification can be divided into frequency response function method [13] and environmental excitation method [14]. As a commonly used modal parameter identification method in engineering, frequency response function method is widely used. However, this kind of method needs

systematic excitation information and response information to identify modal parameters. However, large construction machinery is often attacked by strong winds, waves, earthquakes, and other random loads. For unmeasurable excitation, the traditional modal parameter identification method will lose its effectiveness. Therefore, in this paper, the random subspace method of environmental excitation method is used to identify the modal parameters of the structure, and combined with the strain modal parameter index, the damage identification of aluminum foam sandwich beam is studied. Shi et al. [15–19] made a detailed discussion on the basic theory of stochastic subspace method and did a lot of work on the application of this method from different angles and different aspects.

Ren et al. [20] propose a new damage feature, which can locate the damage of beam structures under different types of excitation by using the system matrices of the forward innovation model based on the covariance-driven stochastic subspace identification of a vibrating system. Cancelli et al. [21] use the SSID method, SEREP method, and PSO technology to identify the damage of simply supported reinforced concrete (RC) beams with good accuracy. Alexander et al. [22] inferred the residual prediction formula based on stochastic method, which is suitable for any damage identification of vibration based.

Compared with the general modal parameter identification methods, that is a structural modal parameter identification method which only depends on the output signal. It does not need to carry on the Fourier transform. It can avoid the leakage caused by the signal truncation, and the method has strong antinoise performance. In this paper, the strain modal parameters are obtained directly by the random subspace modal parameter identification method. The numerical error caused by the difference calculation can be avoided, and the influence of the sensor test error into the calculation can be reduced. In addition, according to the material characteristics of aluminum foam, the analytical formula of bending vibration of foam metal sandwich beam based on modified Timoshenko beam theory is established. The damage location and damage degree of aluminum foam sandwich beam can be accurately identified by two-step method (Figures 1 and 2). In the paper, "Damage Identification of Aluminum Foam Sandwich Beams under Strain Mode Indexes," published in the journal of *Mechanical Design and Manufacturing Engineering*, the author introduces the numerical simulation and theoretical calculation of modal parameter identification of aluminum foam sandwich beams. There is a high degree of coincidence between them. In addition, the superiority of strain modal difference index in structural damage identification is verified.

In the first section, this paper introduces the background and progress of damage identification methods. In the second section, the stochastic subspace method, the improved algorithm of damage identification theory, and the application steps of two-step method are introduced, and the damage identification process of aluminum foam sandwich beams under different cases is simulated by software. In the third section, how to build the test bench and experimental equipment information is introduced, the law between the modal parameters calculated from the test results and the damage is discussed, and the antinoise ability of the stochastic subspace strain modal parameter identification method is studied. Finally, the damage identification effect of the two-step method is summarized.

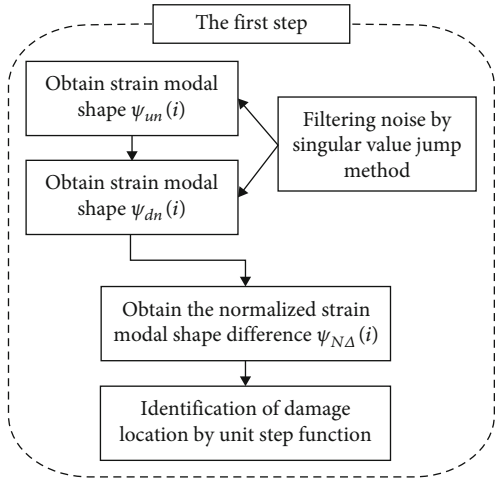

Figure 1: Damage location detection.

2. Theory and Simulation

2.1. Stochastic Subspace Method Theory Driven by Covariance. The covariance-driven stochastic subspace algorithm is based on the properties of the stochastic state space model, and the output data is expressed as a Hankel matrix. The Toeplitz matrix is formed by calculating the covariance sequence of the output data. The system state matrix and the system output matrix are obtained by singular value decomposition of the Toeplitz matrix, and the modal parameters of the structure are obtained. Make the Hankel matrix as [23]

$$\mathbf{H} = \frac{1}{\sqrt{j}} \begin{pmatrix} \mathbf{y}_0 & \mathbf{y}_1 & \cdots & \mathbf{y}_{j-1} \\ \mathbf{y}_1 & \mathbf{y}_2 & \cdots & \mathbf{y}_j \\ \cdots & \cdots & \ddots & \cdots \\ \mathbf{y}_{i-1} & \mathbf{y}_i & \cdots & \mathbf{y}_{i+j-2} \\ \hline \mathbf{y}_i & \mathbf{y}_{i+1} & \cdots & \mathbf{y}_{i+j-1} \\ \mathbf{y}_{i+1} & \mathbf{y}_{i+2} & \cdots & \mathbf{y}_{i+j} \\ \cdots & \cdots & \ddots & \cdots \\ \mathbf{y}_{2i-1} & \mathbf{y}_{2i} & \cdots & \mathbf{y}_{2i+j-2} \end{pmatrix} = \begin{pmatrix} \mathbf{Y}_{0|i-1} \\ \hline \mathbf{Y}_{i|2i-1} \end{pmatrix} = \begin{pmatrix} \mathbf{Y}_p \\ \hline \mathbf{Y}_f \end{pmatrix}. \tag{1}$$

The Hankel matrix is a block matrix containing $2i$ block rows and j columns. Define the output covariance as

$$\mathbf{\Lambda}_i = E\left[\mathbf{y}_{k+i}\mathbf{y}_k^T\right]. \tag{2}$$

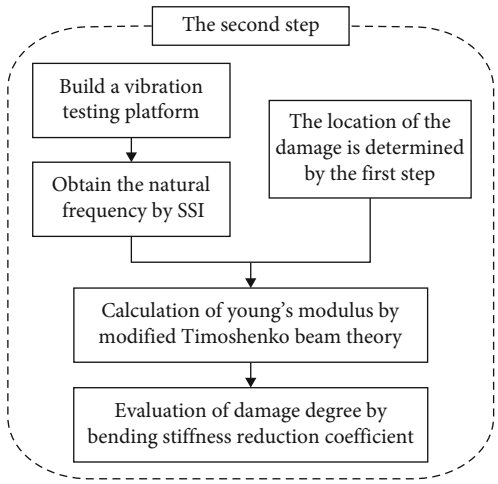

Figure 2: Defect severity detection.

Calculate the output Toeplitz matrix through Equation (2)

$$\mathbf{T}_{l|i} = \mathbf{Y}_f \mathbf{Y}_p{}^T = \begin{pmatrix} \mathbf{\Lambda}_i & \mathbf{\Lambda}_{i-1} & \cdots & \mathbf{\Lambda}_1 \\ \mathbf{\Lambda}_{i+1} & \mathbf{\Lambda}_i & \cdots & \mathbf{\Lambda}_2 \\ \cdots & \cdots & \ddots & \cdots \\ \mathbf{\Lambda}_{2i-1} & \mathbf{\Lambda}_{2i-2} & \cdots & \mathbf{\Lambda}_i \end{pmatrix}, \tag{3}$$

$$\mathbf{T}_{l|i} = \mathbf{\Gamma}_i \mathbf{\Delta}_i. \tag{4}$$

In Equation (4), $\mathbf{\Gamma}_i$ is an extended observable matrix and $\mathbf{\Delta}_i$ is a reverse extended controllable matrix. For $\mathbf{T}_{l|i}$, through singular value decomposition (SVD) and the derivation of the state space equation, we can know

$$\begin{aligned} \mathbf{\Gamma}_i &= \mathbf{U}_1 \mathbf{S}_1{}^{1/2} \mathbf{T}, \\ \mathbf{\Delta}_i &= \mathbf{T}^{-1} \mathbf{S}_1{}^{1/2} \mathbf{V}_1{}^T, \end{aligned} \tag{5}$$

$$\mathbf{T}_{2|i+1} = \mathbf{\Gamma}_i \mathbf{A} \mathbf{\Delta}_i. \tag{6}$$

The output matrix C is equal to the first l row of $\mathbf{\Gamma}_i$.

The system state matrix A can be obtained from Equation (5) and Equation (6). The eigenvalue decomposition of matrix A is as follows:

$$\mathbf{A} = \boldsymbol{\phi} \mathbf{\Lambda} \boldsymbol{\phi}^{-1}, \tag{7}$$

where $\mathbf{\Lambda} = \text{diag}(\lambda_i), i = 1, 2, \cdots, n, \lambda_i$ are the eigenvalues of the discrete-time system. Because the actual system is continuous, the relationship between the eigenvalue λ_{ci} of the continuous-time system and the eigenvalue λ_i of the discrete-time system can be expressed as

$$\lambda_{ci} = \frac{\ln \lambda_i}{\Delta t}. \tag{8}$$

The vibration frequency and modal shape of the system can be expressed as

$$\begin{aligned} f_i &= \frac{|\lambda_{ci}|}{2\pi}, \\ \boldsymbol{\varphi}_i &= \mathbf{C} \boldsymbol{\phi}_i. \end{aligned} \tag{9}$$

In Equation (9), $|\cdot|$ is the length of the complex vector.

2.2. Analytical Solution of Dynamic Parameters of Aluminum Foam Sandwich Beams. On the basis of the Timoshenko beam theory, the influence of momentum of inertia caused by shear deformation on beam vibration is further considered. A modified Timoshenko beam theory can be established. This theory can more truly reflect the vibration characteristics of metal foam.

For the cantilever boundary condition, we know that $\varphi(0) = \Theta(0) = \mu AG\Gamma(l) = \bar{M}(l) = 0$. Substituting which into Equation (B.13), and equation (B.15) until equation (B.17), there are

$$\begin{aligned} \varphi(0) &= b + d = 0, \\ \Theta(0) &= Aa + Bc = 0, \\ \mu AG\Gamma(l) &= \mu AG((A - \alpha)a \cos(\alpha l) - (A - \alpha)b, \\ \sin(\alpha l) &+ (B - \beta)c\text{ch}(\beta l) + (B - \beta)d\text{sh}(\beta l)) = 0, \\ \bar{M}(l) &= EI(-A\alpha\text{asin}(\alpha l) - A\alpha b \cos(\alpha l) \\ &+ B\beta c\text{sh}(\beta l) + B\beta d\text{ch}(\beta l)) = 0. \end{aligned} \tag{10}$$

Rewrite the coefficient of equation (10) into a determinant. According to the linear algebra theory, if there is a nonzero solution to a system of homogeneous linear equations, the determinant composed of the coefficients of the equation must be zero. The numerical solution of frequency can be obtained by MATLAB calculation, and the strain modal shape of aluminum foam sandwich beam under cantilever boundary condition can be obtained by substituting the calculated natural frequency into

$$\begin{aligned} \psi_n(x) = -\frac{h_1}{2}(&-A\alpha\text{asin}(\alpha x) - A\alpha b \cos(\alpha x) \\ &+ B\beta c\text{sh}(\beta x) + B\beta d\text{ch}(\beta x)). \end{aligned} \tag{11}$$

Suppose the thickness of the upper and lower panels of the aluminum foam sandwich beam is t, the elastic modulus and shear modulus are E_{fp} and G_{fp}, respectively, and the thickness of the core is c, and the elastic modulus and shear modulus are E_c and G_c, respectively. It is mentioned in this paper [24] that the equivalent shear elastic modulus and the equivalent elastic modulus of aluminum foam sandwich beams can be expressed as

$$G_{eq} = \frac{G_c(c+t)^2}{c(c+2t)},$$
$$E_{eq} = 6\left(\frac{E_{fp}t(c+t)^2}{(c+2t)^3} + \frac{E_{fp}t^3}{3(c+2t)^3} + \frac{E_c c^3}{6(c+2t)^3}\right). \quad (12)$$

The length, width, panel thickness, and core thickness of the beam are 0.5 m, 0.04 m, 0.003 m, and 0.018 m, respectively. The material of the panel is industrial pure aluminum, elastic modulus $E_{fp} = 72$ GPa, shear modulus $G_{fp} = 26.7$ GPa, Poisson's ratio $\nu_{fp} = 0.35$, and density $\rho_{fp} = 2700\,\text{kg/m}^3$; core material is closed-cell aluminum foam, elastic modulus $E_c = 516$ MPa, shear modulus $G_c = 200$ MPa, Poisson's ratio $\nu_c = 0.29$, and density $\rho_c = 300.27\,\text{kg/m}^3$. Substituting the parameters of aluminum foam sandwich beam into Equation (10) and Equation (12), the first four natural frequencies of aluminum foam sandwich beam are calculated and verified by Ansys Workbench simulation results. In order to save calculation cost, the core is modeled by solid cuboid. The natural frequency is shown in Table 1.

Because the numerical solution of the simulation software is calculated by the Timoshenko beam theory, the numerical solution is different from the analytical solution in the paper. The Timoshenko beam theory lacks a coupling term of shear deformation and moment of inertia. The analytical solution is smaller, and the error increases with the increase of modal order.

2.3. Numerical Simulation. To explore the relationship between damage location, damage degree, damage quantity, and modal parameters of aluminum foam sandwich beam, the first three-order strain modal parameters of the structure are extracted and discussed in the simulation. A total of six different cases are set in the simulation, which are distinguished according to different locations and different degrees of damage.

The beam model is divided into 100 units. Taking the cantilever boundary as an example, the damage is set in unit 35 or 65 of the sandwich beam. The specific parameters of each case of different cases obtained by simulation software are shown in Table 2.

The method of reducing the bending stiffness of the unit is used to simulate the damage, and the first three natural frequencies of the cantilever beam under different cases are extracted, as shown in Table 3.

In Table 3, δ_1 represents the error between the analytical solution and the numerical solution of the natural frequency of healthy beams. δ_2 to δ_6 represent the relative change rate of the natural frequency of case 2 with that of healthy beam, up to the natural frequency of case 6 with that of healthy beam, respectively.

In Table 3, it can be found that the higher the natural frequency order, the greater the relative change rate of the natural frequency, but the change rate of the third natural frequency in some cases is smaller than that of the first two, so it is necessary to identify the damage information by combining multiorder frequencies. The greater the amount of damage, the greater the rate of change of frequency. However, the frequency is not sensitive to the microdamage of aluminum foam sandwich beam, so the natural frequency can only identify the common damage of aluminum foam sandwich beam, while the identification of microdamage and damage location needs the help of modal shape.

Table 1: Analytical solution for the first four natural frequencies (Hz).

Modal order	1	2	3	4
Analytical solution	97.15	404.19	860.33	1312.34
Simulation solution	97.64	447.85	973	1509

Table 2: Model damage cases.

Case	Damage quantity	Damage location	Damage degree
1	Health	/	/
2	Single damage	35	4%
3	Single damage	35	12%
4	Single damage	65	4%
5	Single damage	65	12%
6	Double damage	35, 65	4%, 12%

Table 3: Numerical solution of the first 4 natural frequencies of each case.

Case	Modal order		
	1	2	3
1	97.636	447.85	973
δ_1	0.498%	9.749%	11.580%
2	97.631	447.81	972.89
δ_2	-0.005%	-0.009%	-0.011%
3	97.621	447.73	972.63
δ_3	-0.015%	-0.027%	-0.038%
4	97.634	447.82	973
δ_4	-0.002%	-0.007%	0.000%
5	97.629	447.77	972.99
δ_5	-0.007%	-0.018%	-0.001%
6	97.624	447.73	972.88
δ_6	-0.012%	-0.027%	-0.012%

The software Ansys Workbench 11.9 needs to define the path to derive the data when obtaining the modal shape of beam units. In the actual test, the strain gauge is usually pasted on the upper surface of the beam, so the path is defined in the position of the longitudinal symmetry axis on the upper surface of the aluminum foam sandwich beam. The point-line diagram is drawn through the derived modal shape data, and the displacement modal shape is shown in Figure 3.

The amplitude of the displacement modal shape of the aluminum foam sandwich beam is 78.625 mm, which is submerged because the damage data is too small. It can be seen that the displacement modal shape is not sensitive to

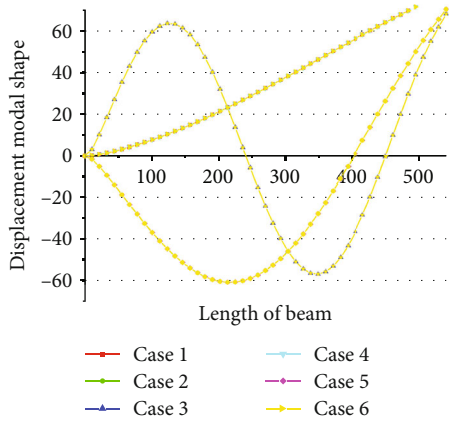

Figure 3: First three displacement modal shapes of each case.

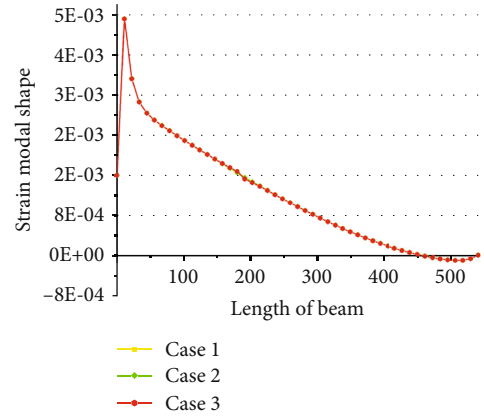

Figure 4: The first-order strain modal shape curve of the 35th unit after damage.

microdamage. In order to amplify the damage information, the strain modal shape of aluminum foam sandwich beams is extracted.

In Figure 4, the amplitude of strain modal shape is 4.72*E*-3. It can be found that the sensitivity of strain modal shape to damage identification is better than that of displacement modal shape, but it is also not significant enough. In the following, the strain modal shape of the damaged beam minus that of the healthy beam is used to amplify the damage information to improve the identification efficiency.

The strain modal shape difference is divided into single damage and double damage situations, as shown in Figures 5 and 6. It is found from the figure that each order strain modal shape difference is more sensitive to damage identification of unit 35 than that of unit 65. The identification effect of the first two-order strain modal shape difference is very good, but the amplitude of the third-order strain modal shape difference of unit 65 is very small, which is a discrepancy from that of the third strain modal shape difference of unit 35. Obviously, this will affect the identification accuracy of the damage degree information. The strain modal shape difference of double damage corresponds to the sum of single damage data at different locations. In the situation of double damage, the amplitude of the third strain modal shape difference is -4.85*E*-4 in unit 35 with damage amount of 4%, and that is 1.4*E*-4 in unit 65 with damage amount of 12%. The third strain modal shape difference is not sensitive to unit 65 damage with damage amount of 12%. Thus, it can be seen that the effect of damage identification only through a certain order of modal shapes is not accurate enough.

2.4. Technical Route. In this paper, aiming at aluminum foam, taking the beam model as the research object, the strain modal shape index is used to locate the damage location, and a modified Timoshenko beam theory is established to evaluate the damage degree. The method includes two steps: the first step is to detect the location of the damage, and the second step is to confirm the severity of the damage by the location of the damage and the evaluation equation. Step of defect location detection and step of defect severity detection are shown in Figures 1, and 2, respectively.

3. Experimental Verification

This experiment is tested by the power testing equipment invented by Jiangsu Donghua Test Technology Co., Ltd. The equipment and software used are shown in Table 4. The experimental data are collected in the way of single-point excitation and multipoint response.

3.1. Prefabrication of Damaged Beam. In the experiment, the beam is divided into 10 units and installed in the form of cantilever boundary fixed at one end and free at the other end, as shown in Figure 7; the hole crack defects are prefabricated at the panel position of the beam by precision power tools, and the detail view and cross-sectional view of the damage are shown in Figure 8. Two damage points are selected, which are located in unit 3 and unit 6, respectively. Because the exciter cannot be moved on the test bench, the excitation point of the beam is 125 mm from the fixed end of the cantilever beam.

The specific parameters of each case of the specimen are shown in Table 5.

3.2. Experimental Process. The arrangement of the experimental equipment is shown in Figure 9. In the experiment, the white noise excitation is generated by the DH1301 signal generator. It controls the DH40020 electromagnetic exciter causing the cantilever beam to vibrate according to the predetermined signal.

The transverse strain data of the beam are measured by the strain gauge, and the data are collected and recorded by the DH5922D dynamic signal test and analysis system. The modal parameters of aluminum foam sandwich beam are identified by the stochastic subspace method.

3.3. Experimental Results and Analysis. The transverse displacement response of the beam is collected by the accelerometer, and the displacement modal shape is further calculated. The pulse force is applied by a force hammer at the position of unit 6, and the maximum pulse force is about 399.52 N, as shown in Figure 10. In each unit, the maximum acceleration response of the first unit is 994.8835 m/s^2, as shown in Figure 11.

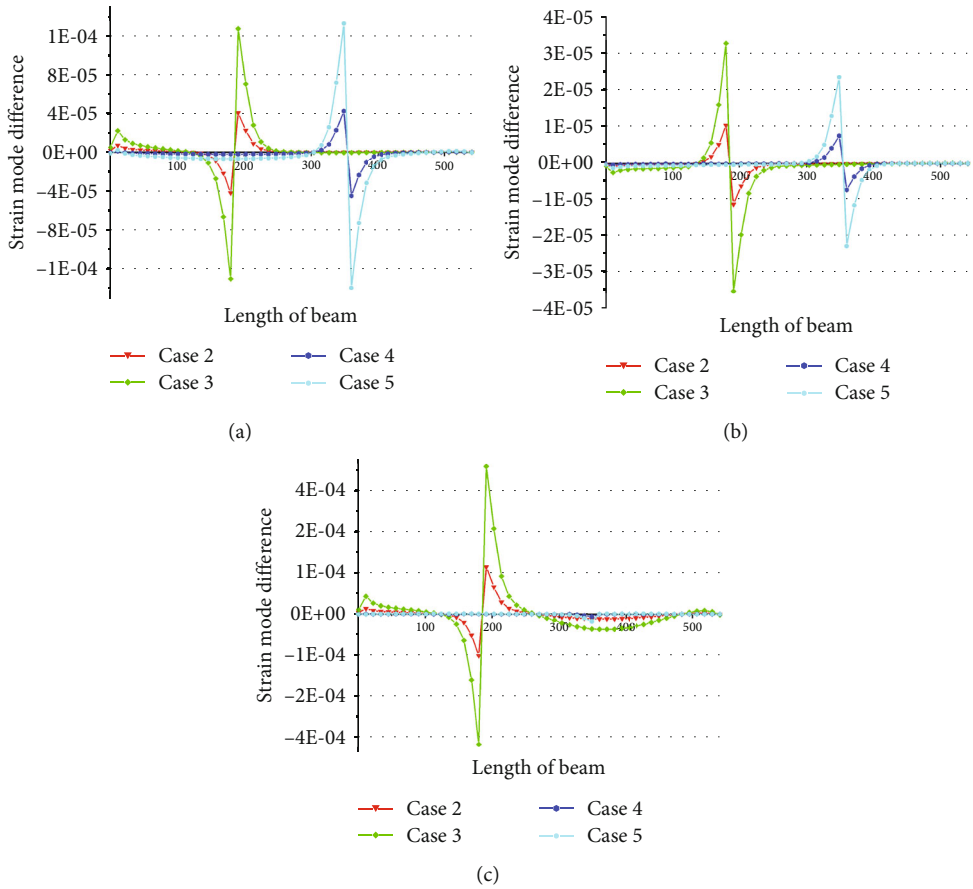

Figure 5: The first three-order strain mode difference curve of single damage case: (a) the first-order strain modal shape difference, (b) the second-order strain modal shape difference, and (c) the third-order strain modal shape difference.

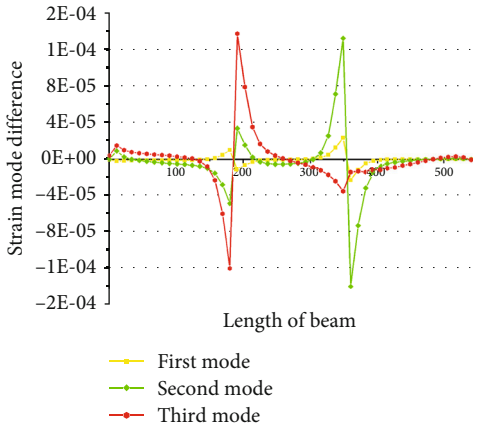

Figure 6: The first three-order strain mode difference curve of double damage case.

In order to discuss the variation of the displacement modal shapes identified by the stochastic subspace method on the different damage cases of the aluminum foam sandwich beam, the first three displacement modal shapes in which the damage is located on the surface of the panel and the damage penetrates from the surface to the core are extracted, as shown in Figure 12.

Among the displacement modal shapes identified by the stochastic subspace method, there are some abrupt changes in each order of modes near unit 3 and unit 8. From the above results, the displacement modal shape has a certain guiding role for the identification of damage location, but the test error is easy to drown the damage information, so the accuracy of microdamage identification of aluminum foam sandwich beam is poor. Compared with the displacement modal shape, the strain modal shape can reflect the local strain of the damage. Usually, the strain modal shape of the damage unit is much larger than the test error. Hereinafter, the damage information of the beam is identified by the strain modal shape of the aluminum foam sandwich beam.

As a damage identification index, strain modal shape has stronger noise and test error robustness than displacement modal shape. The first three strain modal shapes of six kinds of cases are extracted in the experiment. The first three strain modes of each case are divided by the maximum corresponding order modal shape of case 1, respectively, to unify the amplitude ratio of the modal shape, as shown in Figure 13.

From the above results, it is found that the first three strain modal shapes cannot identify the damage information of case 2. Because the strain gauge is too far from the damage position, the strain gauge towards the damage position is

Table 4: Experimental equipment and software.

Name	Type	Specifications	Quantity
Force hammer	LC02	1 m V/N	1
Force transducer	3A102	4 p C/N	1
Electric vibration exciter	DH40020	20 N	1
Piezoelectric accelerometer	1A110E	5.06 m V/(m s^2)	6
Uniaxial strain gauge	BX120-3AA	120 Ω	20
Signal generator	DH1301	0.1 Hz~9999.9 Hz	1
Signal acquisition instrument	DH5922D	±100 mV~±10 V	1
Desktop computer	DELL	\	1
DHDAS analysis software	\	\	1

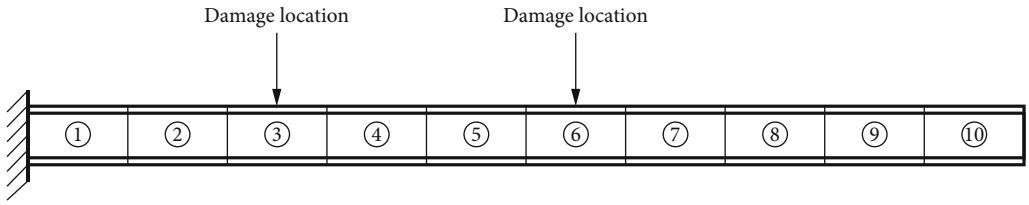

Figure 7: The damage location of the cantilever beam.

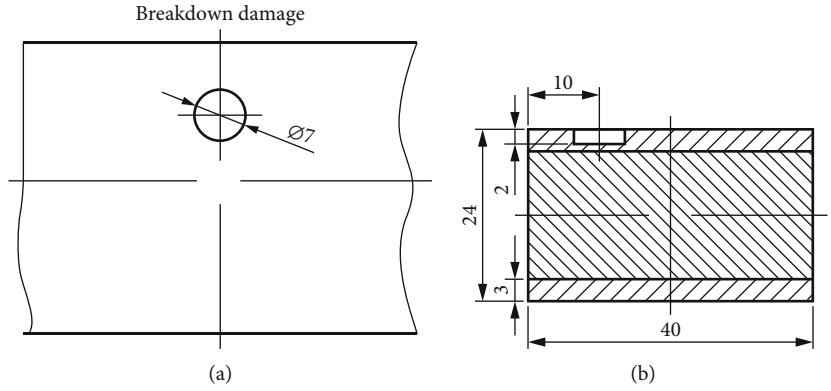

Figure 8: (a) Detail view and (b) cross-sectional view of damage.

Table 5: Experimental case.

Case	Damage quantity	Damage location	Damage degree
Case 1	Zero damage	/	/
Case 2	Single damage	3	2 mm
Case 3	Single damage	3	4 mm
Case 4	Single damage	6	2 mm
Case 5	Single damage	6	4 mm
Case 6	Double damage	3, 6	2 mm, 4 mm

moved 3 mm among subsequent cases. Except for the poor accuracy of damage identification in case 2, the first strain modal shapes from case 3 to case 6 have obvious abrupt changes in the damage location. The modal shape value of the third unit of case 1 is 0.675, the modal shape value of unit 3 of case 3 is 0.792, and the vibration shape value of unit 3 of case 6 is 0.797. Because of noise interference and test errors, some modal shapes cannot distinguish different damage degree information. However, the different damage degree information of unit 6 from case 4 to case 6 can be reflected in the strain modal shape. From the observation of the second strain mode of each case, the modal shape of case 4 has a prominent change in the third unit, and the modal shape of case 5 has a certain collapse in the third unit, which is caused by the test error. The modal shape value of unit 6 of case 4 is larger than that of case 5 and case 6, which does not accord with the actual damage. The modal shape value of unit 6 of case 5 and case 6 is relatively close, but the mutation of the modal shape value of unit 3 of case 6 is not obvious. The third-order strain modal shape in each case is observed. The modal shape disturbance of unit 3 is large, and the accuracy of damage identification is poor. The sudden change of modal shape of unit 6 under cases 4, 5, and 6 is very obvious, but the damage degree

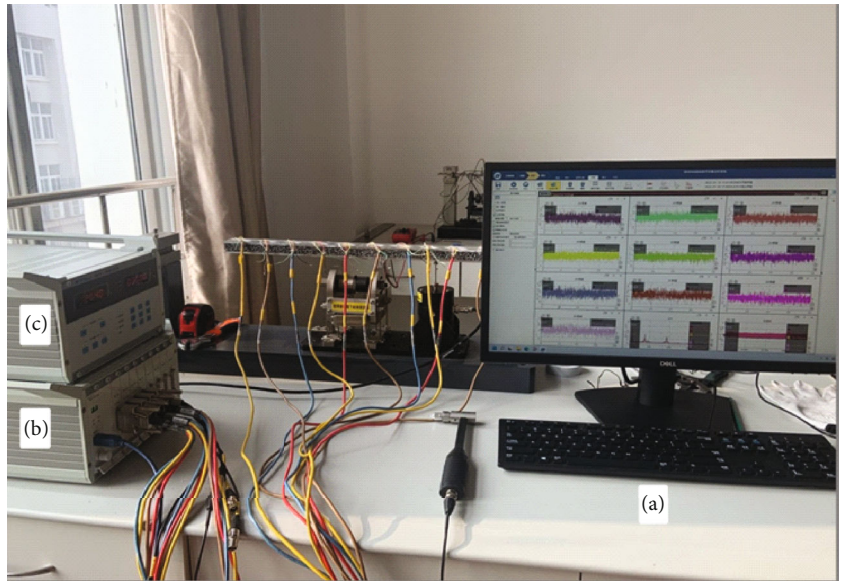

Figure 9: Experiment instruments: a—computer, b—dynamic signal acquisition instrument, and c—signal generator.

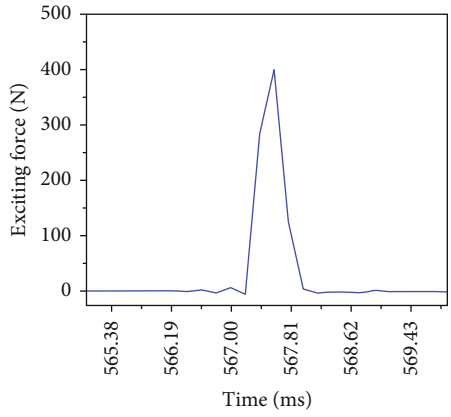

Figure 10: Pulse force time domain signal.

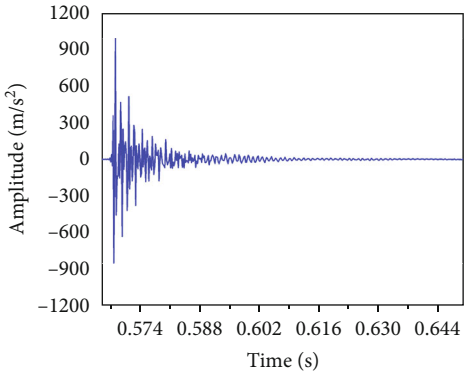

Figure 11: Acceleration time domain response.

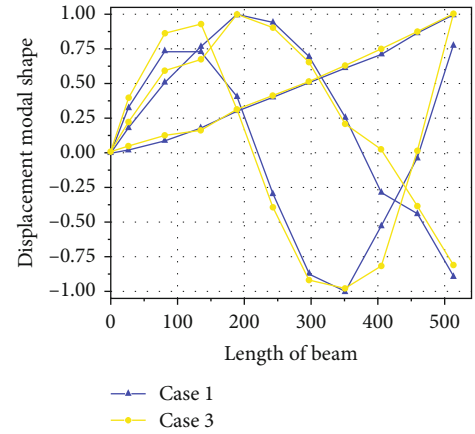

Figure 12: Modal shape recognition by stochastic subspace method.

information reflected is not consistent with the actual damage. In addition, unit 4 of the first- and second-order strain modal shapes in case 4 to case 6 has a certain disturbance, which is due to the fact that the strain response data collected by the strain gauge of unit 4 are not completely cleared in the process of data collection.

Because the strain sensor can only identify the damage in its own region or adjacent areas, for case 2, in addition to arranging more sensors, we can find a strain sensor with wider coverage, such as FBG sensor, which has a larger size and a recognition range of up to meter level, and both ends are welded on the structure, and the stability is good [25–27].

In engineering practice, test errors are everywhere and inevitable. In order to improve the accuracy of damage identification of aluminum foam sandwich beams by strain modal shapes, it is necessary to integrate multiorder modal data for damage identification, and the normalized strain modal shape difference index is proposed, which is marked as $\psi_{N\Delta}(i)$. In order to reflect the damage location information more directly, the threshold is introduced into the damage index, and the enhanced strain modal shape difference

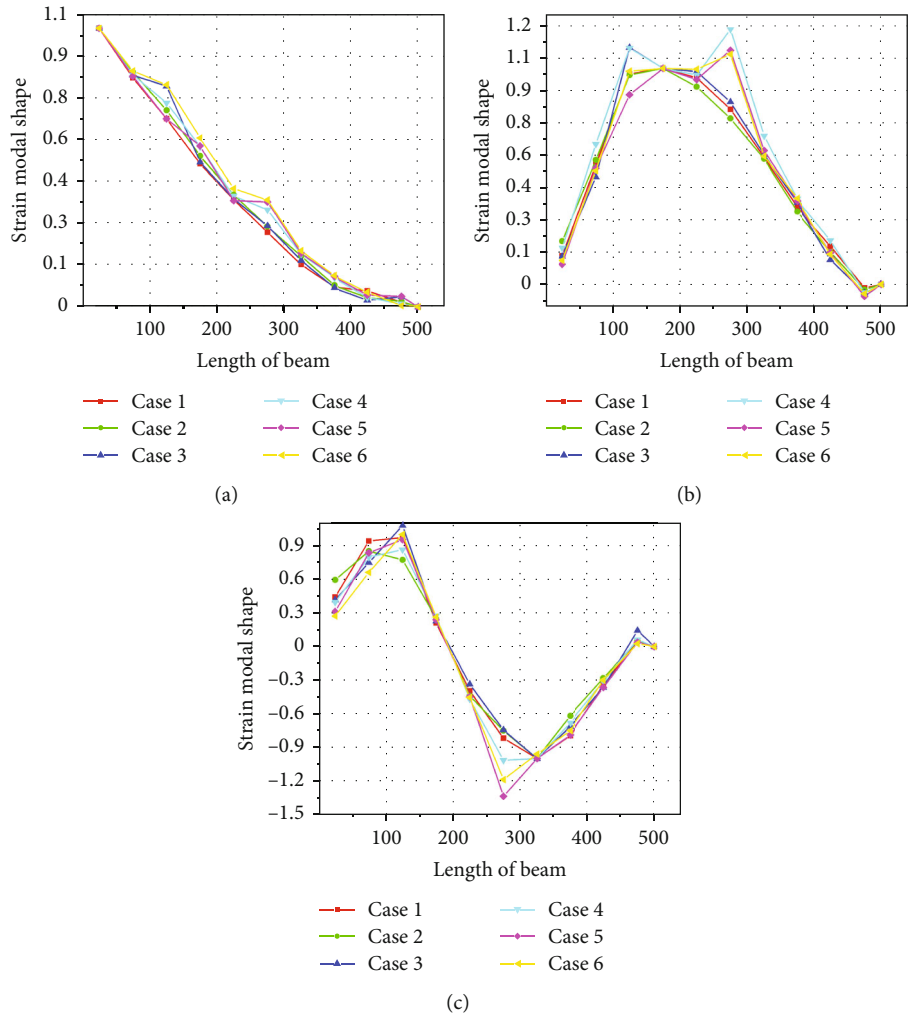

Figure 13: The first three strain modal shapes: (a) first mode; (b) second mode; (c) third mode.

index is established, which is marked as $\psi_{EN\Delta}(i)$. $\psi_{N\Delta}(i)$ and $\psi_{EN\Delta}(i)$ can be expressed as

$$\psi_{N\Delta}(i) = \frac{(1/n)\sum_1^n |\psi_{un}(i) - \psi_{dn}(i)|}{\mathrm{MAX}((1/n)\sum_1^n |\psi_{un}(i) - \psi_{dn}(i)|)},$$

$$\psi_{EN\Delta}(i) = u(\psi_{N\Delta}(i) - \xi), \tag{13}$$

$$u(x) = \begin{cases} 1, x \geq 0, \\ 0, x < 0. \end{cases}$$

In Equation (13), $\psi_{un}(i)$ and $\psi_{dn}(i)$ represent the strain modal shapes before and after the damage of the i unit in the nth order of the aluminum foam sandwich beam, respectively. $u(x)$ is the unit step function, and ξ is the damage threshold. Limited to the length of the article, this paper only draws the normalized strain modal shape difference index and the enhanced strain modal shape difference index of case 6, as shown in Figure 14, and ξ of case 6 is set at 30%.

In case 6, the amplitude of the normalized strain modal difference index of unit 3 and unit 6 is higher, but the amplitude of unit 3 is only 36.33%, and the damage information is easy to be overwhelmed by the test error. The microdamage is more significantly reflected in the first strain modal shape, so the damage location information can be identified by combining the strain modal shape index and the normalized strain modal shape difference index. From the observation of the enhanced strain modal shape difference index in case 6, the damage location information of aluminum foam sandwich beam is very intuitive. Other errors are filtered by introducing damage threshold, and the identification accuracy is very high. The enhanced strain modal shape difference index is helpful to write a program for automatic monitoring. However, neither the normalized strain modal shape difference index nor the enhanced strain modal shape difference index can reflect the structural damage degree information, and the strain modal shape is greatly affected by the test error. In the following, the elastic modulus of the damaged unit is calculated based on the natural frequency analytical formula of the modified Timoshenko beam theory.

The natural frequencies of the first three-order aluminum foam sandwich beams under different cases are

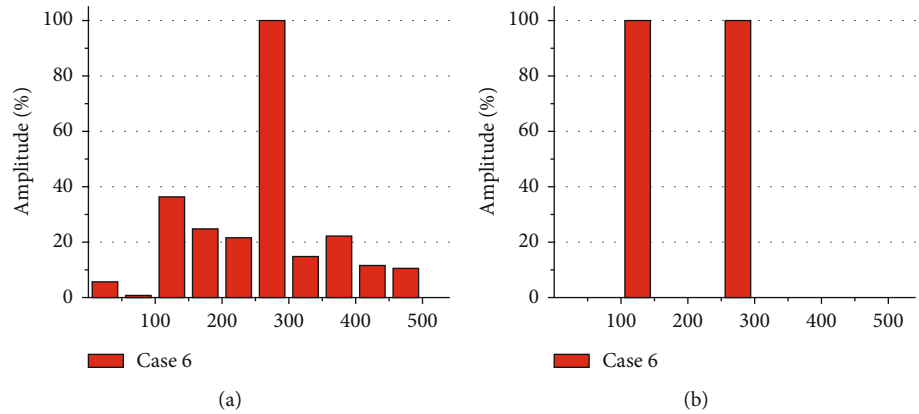

Figure 14: (a) Normalized strain modal shape difference index. (b) Enhanced strain modal shape difference index.

extracted in the strain mode experiment, as shown in Table 6.

In Table 6, it can be found that except for the large difference between the first-order natural frequency of aluminum foam sandwich beam in case 1 and the theoretical and numerical solution of zero damage beam in Table 1, the natural frequency error of other order in case 1 is less than 10%. It is verified that the theory of equivalent bending stiffness and equivalent shear stiffness of sandwich beam in Equation (12) is more accurate. It is speculated that the shear modulus of aluminum foam sandwich beam core is not a constant, and it is considered that the shear modulus increases with the increase of modal order. The first natural frequency of case 1 is 46.235 Hz, which is smaller than the first natural frequency of other cases, which does not accord with the actual situation. Except for the third natural frequency of case 2, the second natural frequency and the third natural frequency of case 1 are larger than those of other cases. In general, if the degree of damage of the structure is greater, the corresponding natural frequency is smaller; if the order is higher, the change of the natural frequency of the damaged beam is greater. In Table 6, the natural frequency of individual damage cases is larger than that of case 1, which is caused by the calculation error of parameter identification algorithm and test error.

Because the first-order natural frequency of case 1 is smaller than that of other cases, the experimental data of the first-order natural frequency are not consistent with the analytical solution in Table 1. In this paper, only the inverse operation of the natural frequencies of the second and third orders of aluminum foam sandwich beams is carried out to solve the damage degree information of the structure. According to the previous inference of shear modulus, in order to unify the analytical solution of natural frequency with the experimental data, the equivalent shear modulus of aluminum foam sandwich beam at the second frequency vibration is taken as 176.29 MPa, and the equivalent shear modulus at the third frequency vibration is taken as 236.08 MPa. Through the MATLAB 2021 operation (Equation (10)), the transcendental equation of the natural frequency of aluminum foam sandwich beam, the elastic

Table 6: Natural frequencies (Hz).

Case	Modal order		
	1	2	3
Case 1	46.235	401.914	940.478
Case 2	55.038	393.532	944.937
Case 3	54.425	387.310	881.190
Case 4	54.920	394.745	937.192
Case 5	54.499	379.999	883.446
Case 6	54.378	377.751	870.759

Table 7: Elastic modulus of each case (GPa).

Case	Modal order	
	2	3
Case 1	4.17	4.17
Case 2	3.76	4.29
Case 3	3.48	2.83
Case 4	3.81	4.07
Case 5	3.20	2.87
Case 6	3.11	2.66

modulus of each case is obtained based on the natural frequency of the damage case, as shown in Table 7.

To observe the elastic modulus of each case, in addition to the elastic modulus calculated by the third natural frequency of case 2, if the damage degree of aluminum foam sandwich beam is greater, the corresponding elastic modulus is smaller. The elastic modulus of case 2 is similar to that of case 4, that of case 3 is similar to that of case 5, and the elastic modulus of case 6 is smaller than that of other cases. By substituting the elastic modulus into the damage conversion coefficient of bending stiffness, the degree of the damage unit is further calculated, as shown in Figure 15.

The damage degree information of aluminum foam sandwich beam obtained by the second natural frequency is observed. The damage depth of case 2 and case 4 is 2 mm, and the damage amount is 10% and 9%, which is more in line with the actual damage. The damage depth of case 3 and case 5 is 4 mm, the degree of damage is 16%

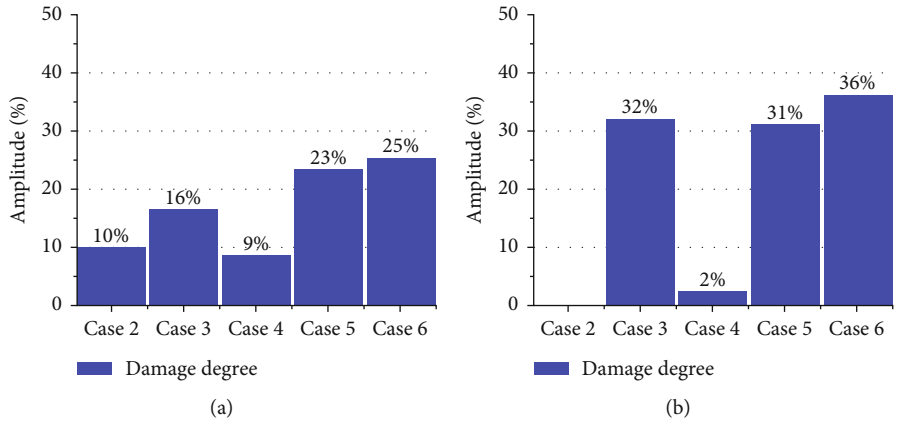

Figure 15: (a) Damage degree information obtained by the 2nd-order natural frequency. (b) Damage degree information obtained by the 3rd-order natural frequency.

and 23%, and the damage of case 6 is 25%. Among them, the damage degree information identified by case 6 is more consistent with the actual damage situation, while the damage degree information identified by case 5 is larger than the actual damage situation. According to the observation of the damage degree information of the aluminum foam sandwich beam obtained from the third natural frequency, the damage degree of case 4 is 2%, the damage degree of case 3 and case 5 is 32% and 31%, respectively, and the damage degree of case 6 is 36%. It is not consistent with the actual damage, and the third natural frequency may be a false frequency.

3.4. Analysis of Antinoise Performance of Stochastic Subspace Strain Modal Parameter Identification Method. The traditional modal parameter identification methods are often affected by the external environmental noise, resulting in a large error between the estimated values and the actual values of the modal parameters of the structure. In structural damage identification, this kind of error is easy to cause damage misdiagnosis, so it is necessary to fully reduce the noise of vibration test data in practical engineering application. Commonly used signal denoising methods are as follows: moving average method, wavelet denoising method, EEMD method, and so on [28–30]. The above methods can restrain the noise to a certain extent, but it will inevitably destroy the original information of the test signal, so there are some limitations in the application. Compared with the traditional modal parameter identification method, the stochastic subspace method has stronger antijamming ability. Because the singular value affected by noise in the singular value of the Toeplitz matrix is close to zero, engineers can filter out most of the noise modes and false modes by determining the rank of the Toeplitz matrix. Limited to the length of the article, in order to study the antinoise ability of stochastic subspace modal parameter identification method, the author adds three kinds of Gaussian white noise of different intensities to the strain response data of case 6 by MATLAB self-program to simulate the external noise interference. In order to meet the needs of the project, a larger noise intensity is selected, which is 1.5 times, 4 times, and

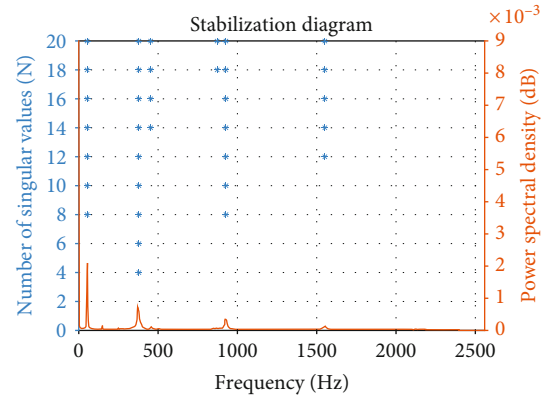

Figure 16: Stabilization diagram and power spectral density diagram.

Table 8: Natural frequencies under different levels of noise interference (Hz).

Case	Modal order		
	1	2	3
1.5 times the noise	54.47	377.79	929.93
4 times the noise	55.41	376.95	929.10
9 times the noise	54.38	377.60	929.33

9 times the signal intensity, respectively. The corresponding signal-to-noise ratio (SNR) can be calculated according to the following equation [31]:

$$\mathrm{SNR} = 10 \lg \left(\frac{\sum_1^N (y_{oi})^2}{\sum_1^N (y_{ni})^2} \right). \tag{14}$$

In Equation (14), y_{oi} is the discrete data of the original signal, and y_{ni} is the discrete data of the noise signal. According to Equation (14), the signal-to-noise ratio of the signal with noise is -1.761 dB, -6.021 dB, and -9.542 dB, respectively. The Gaussian white noise with different signal-to-

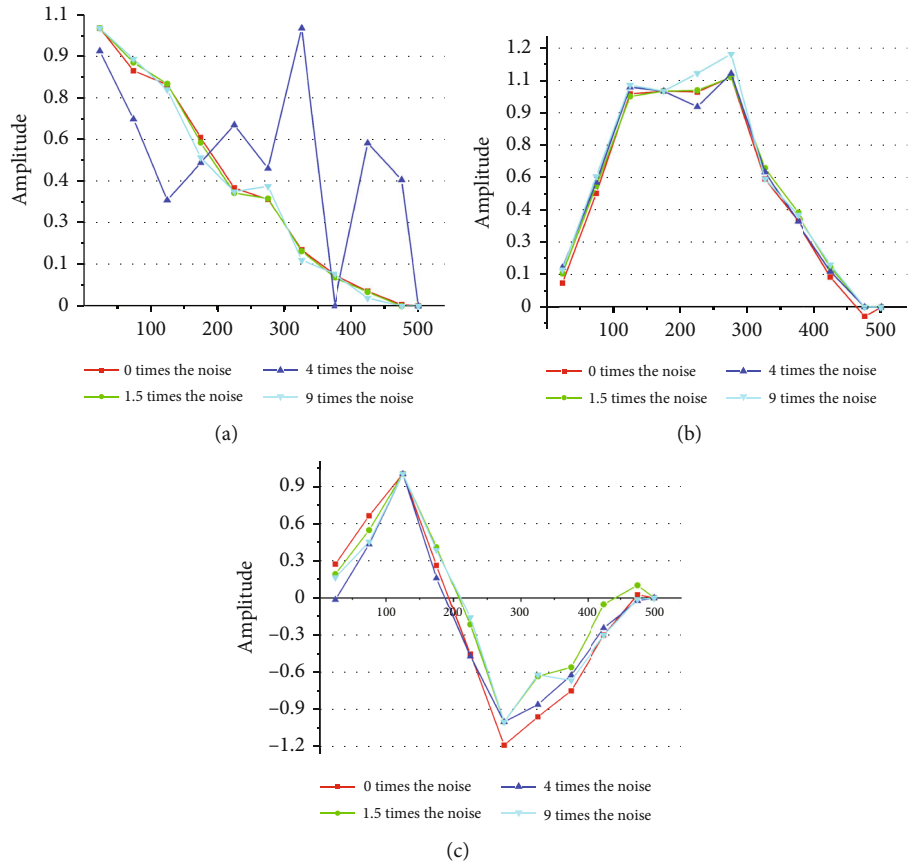

Figure 17: The first three-order strain modal shapes under different levels of noise interference.

noise ratios can be obtained through the awgn function; for example, awgn $(y(:,1\mathrm{SNR},\text{'measured'}))$ represents the addition of a Gaussian white noise at a certain ratio based on the actual power of the signal to the data from the first column to the nth column of the measuring point in the y signal matrix. In the following article, the signal after adding noise is imported into the self-programming of the stochastic subspace method. The order of the system is judged according to the frequency stability diagram and the power spectral density function of the response signal, and the first three strain modal parameters of case 6 are identified. The stabilization diagram and power spectral density diagram of the signal after adding 1.5 times Gaussian white noise are shown in Figure 16.

In Figure 16, the left longitudinal axis is the number of singular values of the Toeplitz matrix, the right longitudinal axis is the power spectral density function of the signal, and the transverse axis is the natural frequency of the structure. When the number of singular values is 12, the first four natural frequencies of the signal can be reflected in the stability diagram. When the number of singular values exceeds 12, one false mode is generated near 500 Hz and one near 1000 Hz. Therefore, the noise or false modes caused by the algorithm can be filtered by selecting the appropriate system order. In the power spectral density diagram, it can be observed that the signal power spectral density has a peak at the first four natural frequencies, and the power spectral density decreases with the increase of the order. The accuracy of the stability diagram can be verified from the shape of the power spectral density function curve at the resonance frequency of the structure. According to the sampling frequency of the signal and the relevant experience, the number of block rows of the Hankel matrix i is 50 and the system order N is 12. Through calculation, the natural frequencies of aluminum foam sandwich beams under various noise states are shown in Table 8.

In Table 8, it is found that the first three natural frequencies of the structure in each noise state are very similar, except the third-order natural frequency, and the other order frequencies are similar to the natural frequencies of case 6 in the noise-free state in Table 3. From the above analysis, it can be seen that the stochastic subspace strain modal parameter identification method has a strong antinoise ability in identifying the natural frequency of the structure. The third-order natural frequency in Table 6 is affected by the number of orders of the system and is a false mode. In fact, the damage degree information of aluminum foam sandwich beam identified by the third natural frequency is smaller than that in Figure 15(b). The third natural frequency data in Table 8 further verify the accuracy of using the frequency determinant based on the modified Timoshenko beam theory to identify the damage degree information of foam metal sandwich structure. By calculating the strain modal shapes under different noise states and comparing them with those

of case 6 in Figure 13, the antinoise performance of random subspace method in strain mode identification is discussed. The strain modal shapes under different noise intensity interference states are shown in Figure 17.

As observed in Figure 17, the first three strain modal shapes with noise are basically the same as those without noise, so the random subspace strain mode parameter method has strong antinoise ability in identifying the strain modal shapes of the structure. In Figure 17(a), because the Gaussian white noise has strong randomness and the noise power is too high, the original information of the signal is damaged to a certain extent after adding 4 times noise, and the signal in this noise state cannot accurately calculate the first strain modal shape of the structure. In Figure 17(b), the second strain modal shape vector of each case is very close, and it can be found that there is a significant abrupt change in the strain modal shape of unit 3 and unit 6 of aluminum foam sandwich beam. In Figure 17(c), the third strain modal shape in each noise state is relatively close, and the damage location information of the third unit can be reflected, while the strain modal shape disturbance of the unit 6 position is larger, which has a certain abrupt change compared with the third strain modal shape in the healthy state. By increasing the noise intensity, it is found that in the identification process of strain mode parameters under the interference of higher noise intensity, the natural frequency gradually deviates from the real value with the increase of noise intensity, and the strain modal shape will produce large errors. Finally, as an engineering application, the stochastic subspace strain modal parameter identification method in this paper has met the needs of most projects.

4. Conclusion

According to the vibration experiments, the effectiveness of the stochastic subspace method in damage identification of aluminum foam sandwich beams is verified. Except for the fundamental frequency, the analytical solution of the natural frequency of the modified Timoshenko beam theory is basically consistent with the simulation and experimental values. In the experiment, except that the damage in case 2 exceeds the induction range of the strain gauge and the strain modal shape does not identify the damage location, the damage location information of the aluminum foam sandwich beam can be well identified under other cases, but the damage degree information is easily disturbed by errors. The normalized strain modal shape index can integrate multiorder modal parameters for damage identification, and the enhanced strain modal shape index can filter the error and highlight the damage location information by introducing the damage threshold. The damage degree information identified by the two-step method can guide the engineering practice to a certain extent and can reflect the damage degree information to a great extent. Finally, taking the strain response data of case 6 as an example, three kinds of noise of different intensities are added to the signal to identify the strain modal parameters, and the excellent antinoise performance of the stochastic subspace strain modal parameter identification method is proved. The fault diagnosis technology of foam metal structure is a complex and comprehensive problem, and the following aspects need to be further studied:

(1) The various cases of the aluminum foam sandwich beam are numerically simulated by using the simulation software, the corresponding displacement modal shapes and strain modal shapes are obtained, and the law between modal shapes and damage is discussed

(2) By studying the modified Timoshenko beam theory and combining with the equivalent modulus equation, a relatively perfect dynamic equation of metal foam structure is established. The equation can reflect the accuracy of the experimental data, and it is the key to identify the degree of damage in the second step

(3) In the experiment, the single damage and double damage information of aluminum foam sandwich beam are effectively identified by the two-step method, and this method has strong antinoise ability

(4) The two-step method can improve the automatic identification ability of the operation mode analysis method. It is verified by experiments that the accurate modal parameters can be calculated under random excitation, and the all-weather online monitoring of in-service machinery in the field can be realized

Appendix

A. Mathematical Principle of Stochastic Subspace Method

In practical engineering applications, because the input of the system cannot be measured, it is usually assumed to be a white noise signal, so the random discrete-time state space model can be expressed as

$$\begin{cases} \mathbf{x}_{k+1} = \mathrm{A}\mathbf{x}_k + \boldsymbol{\omega}_k, \\ \mathbf{y}_k = \mathrm{C}\mathrm{x}_k + \boldsymbol{\nu}_k. \end{cases} \tag{A.1}$$

Assuming that the above system is asymptotically stable, observable, and controllable, in the theory of control science, observability means that under the action of a certain control signal, it is observed that the output of the system can uniquely determine the initial state $\mathbf{x}_0$ of the system over a period of time. Controllability means that the allowable input can be found and any initial state $\mathbf{x}_0$ can be transferred to the origin of the state space over a period of time. Suppose that noise $\boldsymbol{\omega}_k$ and $\boldsymbol{\nu}_k$ are white noise with zero mean, that is, $E[\boldsymbol{\omega}_k] = 0$ and $E[\boldsymbol{\nu}_k] = 0$, then there is a covariance matrix:

$$E\left(\begin{bmatrix} \boldsymbol{\omega}_p \\ \boldsymbol{\nu}_p \end{bmatrix} \cdot \left[\boldsymbol{\omega}_q{}^T \boldsymbol{\nu}_q{}^T\right]\right) = \begin{bmatrix} \mathbf{Q}, \mathbf{S} \\ \mathbf{S}^T, \mathbf{R} \end{bmatrix} \delta(\mathbf{p} - \mathbf{q}). \tag{A.2}$$

In Equation (A.2), E is the expectation factor, δ is the unit pulse function, $\boldsymbol{\omega}_p$ and $\boldsymbol{\omega}_q$ represent the process noise at p and q time, respectively, and $\boldsymbol{\nu}_p$ and $\boldsymbol{\nu}_q$ denote the measurement noise at p and q time, respectively. The stochastic subspace method identification system can be shown in Figure 18.

A stochastic process is a stationary process assumed to be zero mean, that is, $E[\mathbf{x}_k \mathbf{x}_k{}^T] = \boldsymbol{\Sigma}$ and $E[\mathbf{x}_k] = 0$, where $\boldsymbol{\Sigma}$ is independent of time t. $\boldsymbol{\omega}_k$ and $\boldsymbol{\nu}_k$ are not related to the actual state x_k at the same time, that is, $E[\mathbf{x}_k \boldsymbol{\omega}_k{}^T] = 0$, and $E[\mathbf{x}_k \boldsymbol{\nu}_k{}^T] = 0$.

Definition:

$$\begin{cases} \mathrm{G} = \mathrm{E}\left[\mathbf{x}_{k+1}\, \mathbf{y}_k{}^T\right], \\ \boldsymbol{\Lambda}_i = \mathrm{E}\left[\mathbf{y}_{k+i}\, \mathbf{y}_k{}^T\right]. \end{cases} \tag{A.3}$$

The self-covariance matrix $\boldsymbol{\Sigma}$ of the state vector can be expressed as

$$\begin{aligned} \boldsymbol{\Sigma} &= E\left[(\mathbf{A}\mathbf{x}_{k-1} + \boldsymbol{\omega}_{k-1})(\mathbf{A}\mathbf{x}_{k-1} + \boldsymbol{\omega}_{k-1})^T\right] = \mathbf{A}E\left[\mathbf{x}_{k-1}\mathbf{x}_{k-1}{}^T\right]\mathbf{A}^T \\ &\quad + \mathbf{A}E\left[\mathbf{x}_{k-1}\boldsymbol{\omega}_{k-1}{}^T\right] + E\left[\boldsymbol{\omega}_{k-1}\mathbf{x}_{k-1}{}^T\right]\mathbf{A}^T + E\left[\boldsymbol{\omega}_{k-1}\boldsymbol{\omega}_{k-1}{}^T\right] \\ &= \mathbf{A}\boldsymbol{\Sigma}\mathbf{A}^T + \mathbf{Q}. \end{aligned} \tag{A.4}$$

The covariance matrix $\mathbf{G}$ of the state vector and the output vector can be expressed as

$$\begin{aligned} \mathbf{G} &= E\left[(\mathbf{A}\mathbf{x}_k + \boldsymbol{\omega}_k)(\mathbf{C}\mathbf{x}_k + \mathbf{v}_k)^T\right] = \mathbf{A}E\left[\mathbf{x}_k\mathbf{x}_k{}^T\right]\mathbf{C}^T + \mathbf{A}E\left[\mathbf{x}_k\mathbf{v}_k{}^T\right] \\ &\quad + E\left[\boldsymbol{\omega}_k\mathbf{x}_k{}^T\right]\mathbf{C}^T + E\left[\boldsymbol{\omega}_k\mathbf{v}_k{}^T\right] = \mathbf{A}\boldsymbol{\Sigma}\mathbf{C}^T + \mathbf{S}. \end{aligned} \tag{A.5}$$

The covariance matrix $\boldsymbol{\Lambda}_0$ of the output vector can be expressed as

$$\begin{aligned} \boldsymbol{\Lambda}_0 &= E\left[(\mathbf{C}\mathbf{x}_k + \mathbf{v}_k)(\mathbf{C}\mathbf{x}_k + \mathbf{v}_k)^T\right] = \mathbf{C}E\left[\mathbf{x}_k\mathbf{x}_k{}^T\right]\mathbf{C}^T + \mathbf{C}E\left[\mathbf{x}_k\mathbf{v}_k{}^T\right] \\ &\quad + E\left[\mathbf{v}_k\mathbf{x}_k{}^T\right]\mathbf{C}^T + E\left[\mathbf{v}_k\mathbf{v}_k{}^T\right] = \mathbf{C}\boldsymbol{\Sigma}\mathbf{C}^T + \mathbf{R}, \\ \boldsymbol{\Lambda}_i &= E\left[(\mathbf{C}\mathbf{x}_{k+i} + \mathbf{v}_{k+i})(\mathbf{C}\mathbf{x}_k + \mathbf{v}_k)^T\right] \\ &= E\left[\mathbf{C}\left(\mathbf{A}^i\mathbf{x}_k + \mathbf{A}^{i-1}\mathbf{w}_k + \mathbf{A}^{i-2}\mathbf{w}_{k+1} + \cdots + \mathbf{A}\mathbf{w}_{k+i-2}\right.\right. \\ &\quad \left.\left. + \mathbf{w}_{k+i-1} + \mathbf{v}_{k+i}\right)(\mathbf{C}x_k + \mathbf{v}_k)^T\right] = \mathbf{C}\mathbf{A}^i E\left[\mathbf{x}_k\mathbf{x}_k{}^T\right]\mathbf{C}^T \\ &\quad + \mathbf{C}\mathbf{A}^{i-1}E\left[\mathbf{w}_k\mathbf{v}_k{}^T\right] = \mathbf{C}\mathbf{A}^{i-1}\left(\mathbf{A}\boldsymbol{\Sigma}\mathbf{C}^T + \mathbf{S}\right) = \mathbf{C}\mathbf{A}^{i-1}\mathbf{G}. \end{aligned} \tag{A.6}$$

From the above analysis, it can be concluded that

$$\begin{cases} \Sigma = \mathbf{A}\boldsymbol{\Sigma}\mathbf{A}^T + \mathrm{Q}, \\ \mathrm{G} = \mathbf{A}\boldsymbol{\Sigma}\mathbf{C}^T + \mathrm{S}, \\ \boldsymbol{\Lambda}_0 = \mathbf{C}\boldsymbol{\Sigma}\mathbf{C}^T + \mathrm{R}, \end{cases} \tag{A.7}$$

$$\boldsymbol{\Lambda}_i = \mathbf{C}\mathbf{A}^{i-1}\mathbf{G}. \tag{A.8}$$

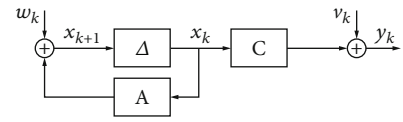

Figure 18: Aluminum foam sandwich beam model.

The $\boldsymbol{\Lambda}_0$ and formula (A.8) in formula (A.7) describe the relationship between output covariance matrix, system state matrix, and system output matrix in mathematical principle and demonstrate the feasibility of solving random identification problem. The stochastic subspace modal parameter identification method deduces the state vector $\mathbf{x}_k$ of the system through the output data, substitutes the state vector and output data into the system state Equation (A.1), and calculates the system matrices **A**, **C**, **Q**, **R**, and **S**. Thus, the modal parameters of the system are obtained.

B. The Derivation Process of Vibration Equation of Cantilever Beam

Because the moment of inertia caused by shear deformation needs to be taken into account in the modified Timoshenko beam theory, the moment of inertia term $\rho I(\partial^2\theta/\partial t^2)dx$ is changed into $\rho I(\partial^2(\theta - \gamma)/\partial t^2)dx$.

According to the mechanics of materials, we can know the expression of shear angle:

$$\gamma = \frac{Q}{\mu AG}, \tag{B.1}$$

where μ is the shear coefficient of the beam section. In this paper, the classical definition of the shear coefficient of the beam with a rectangular section is adopted, and μ is taken as $(10(1+\upsilon))/(12+11\upsilon)$, and υ is Poisson's ratio of the material. Because $\gamma = \theta - (\partial y/\partial x)$, the shear force Q can be rewritten as

$$Q = \mu AG\left(\theta - \frac{\partial y}{\partial x}\right). \tag{B.2}$$

According to the mechanics of materials, the bending moment can be expressed as

$$M = EI\frac{\partial \theta}{\partial x}. \tag{B.3}$$

According to Figure 19, the force balance equation in the y direction and the moment balance equation for the centroid of the section can be listed:

$$-\rho A\frac{\partial^2 y}{\partial t^2}\mathrm{d}x + Q - q(x,t)\mathrm{d}x - \left(Q + \frac{\partial Q}{\partial x}\mathrm{d}x\right) = 0, \tag{B.4}$$

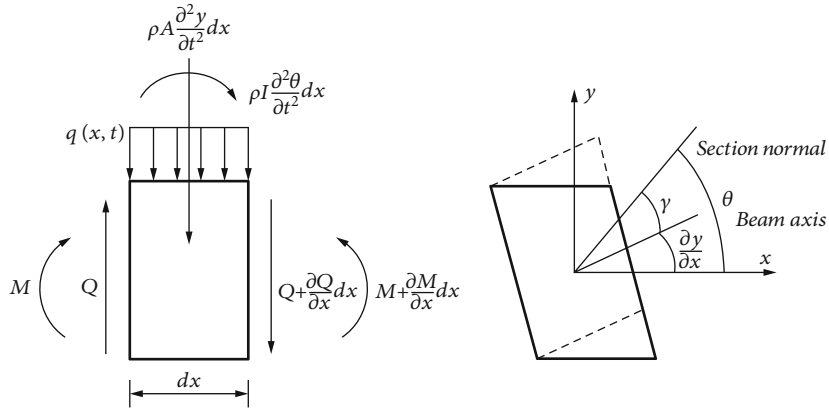

Figure 19: The Timoshenko beam unit force diagram.

$$-\rho I\frac{\partial^2(\theta-\gamma)}{\partial t^2}\mathrm{d}x - M + \left(M+\frac{\partial M}{\partial x}\mathrm{d}x\right) - \left(Q+\frac{\partial Q}{\partial x}\mathrm{d}x\right)\frac{\mathrm{d}x}{2} - Q\frac{\mathrm{d}x}{2} = 0. \tag{B.5}$$

Substitute formula (B.2) to formula (B.4). Both sides of the equation are divided by dx, omitting the second-order small quantity of the formula (13). Substitute formula (B.3) to formula (B.5) and get after transposing the item:

$$\rho A\frac{\partial^2 y}{\partial t^2} + q(x,t) + \mu AG\left(\frac{\partial\theta}{\partial x} - \frac{\partial^2 y}{\partial x^2}\right) = 0, \tag{B.6}$$

$$-\rho I\frac{\partial^2(\theta-\gamma)}{\partial t^2} + EI\frac{\partial^2\theta}{\partial x^2} - \mu AG\left(\theta - \frac{\partial y}{\partial x}\right) = 0. \tag{B.7}$$

The two ends of the equation of formula (B.6) are synchronously divided by μAG. According to the information of cross-section angle, the $(\theta-\gamma)$ in equation (B.7) is replaced by $\partial y/\partial x$, and equation (B.6) and equation (B.7) are derived synchronously to x and get after transposing the item:

$$\frac{\partial\theta}{\partial x} = \frac{\partial^2 y}{\partial x^2} - \frac{q(x,t)}{\mu AG} - \frac{\rho}{\mu G}\frac{\partial^2 y}{\partial t^2}, \tag{B.8}$$

$$\rho I\frac{\partial^4 y}{\partial x^2\partial t^2} - EI\frac{\partial^3\theta}{\partial x^3} + \mu AG\left(\frac{\partial\theta}{\partial x} - \frac{\partial^2 y}{\partial x^2}\right) = 0. \tag{B.9}$$

Substitute formula (B.8) to formula (B.9) and get after transposing the item:

$$EI\frac{\partial^4 y}{\partial x^4} + \rho A\frac{\partial^2 y}{\partial t^2} - \rho I\left(\frac{\partial^4 y}{\partial x^2\partial t^2} + \frac{E}{\mu G}\frac{\partial^4 y}{\partial x^2\partial t^2}\right) = \frac{\partial^2 q(x,t)}{\mu AG\partial x^2} - q(x,t). \tag{B.10}$$

In Equation (B.10), it can be found that differential vibration equation of the modified Timoshenko beam loses a coupling term of shear deformation and moment of inertia, which is caused by the mutual cancellation of the moment of inertia caused by shear deformation.

Let $n(t) = e\sin(\omega t+\eta) + f\cos(\omega t+\eta)$; then, $y = \varphi(x)\,n(t)$. The method of separating variables is used to solve equation (B.10). Because the modal analysis is carried out in the case of free vibration, let $q(x,t) = 0$. The following results can be obtained:

$$\frac{EI}{\rho A}\bullet\frac{\varphi(x)^{(4)}}{\varphi(x) - ((I/A) + (EI/\mu AG))\varphi(x)^{(2)}} = -\frac{n(t)^{(2)}}{n(t)}. \tag{B.11}$$

Because the function $\varphi(x)$ and the function $n(t)$ are independent of each other, make $\sqrt{EI/\rho A} = p$. The left end of equation (B.11) can be rewritten as

$$\varphi(x)^{(4)} + \left(\frac{I}{A} + \frac{EI}{\mu AG}\right)\frac{\omega^2}{p^2}\varphi(x)^{(2)} - \frac{\omega^2}{p^2}\varphi(x) = 0. \tag{B.12}$$

Let $((I/A) + (EI/\mu AG))(\omega^2/p^2) = h^2$, $(\omega^2/p^2) = k^2$ in equation (B.12). Write down the characteristic equation of equation (B.12) as $\lambda^4 + h^2\lambda^2 - k^2 = 0$. The characteristic roots of equation (B.12) are a pair of conjugate imaginary roots $\pm\alpha i$ and a pair of unequal real roots $\pm\beta$. The general solution is

$$\alpha = \sqrt{\sqrt{\left(\frac{h^2}{2}\right)^2 + k^2} + \frac{h^2}{2}},$$

$$\beta = \sqrt{\sqrt{\left(\frac{h^2}{2}\right)^2 + k^2} - \frac{h^2}{2}},$$

$$\varphi(x) = a\sin(\alpha x) + b\cos(\alpha x) + c\mathrm{sh}(\beta x) + d\mathrm{ch}(\beta x). \tag{B.13}$$

Because the beam is affected by shear deformation, the angular modal shape is no longer the first-order partial derivative function of displacement modal shape $\varphi(x)$ to x. Equation (B.6) makes a first-order partial derivative of x

synchronously at both ends. The relationship between the total rotation angle of the beam section and the displacement in the bending vibration equation can be obtained by substituting the result $\partial^2\theta/\partial x^2$ into equation (B.7), which can be expressed as

$$\theta = -\rho I \frac{(1 + (E/\mu G))}{\mu AG} \bullet \frac{\partial^3 y}{\partial x \partial t^2} + \frac{EI}{\mu AG} \bullet \frac{\partial^3 y}{\partial x^3} + \frac{\partial y}{\partial x}. \quad \text{(B.14)}$$

Substituting h^2, $y = \varphi(x)n(t)$, and $\theta = \Theta(x)n(t)$ into Equation (B.14), the corner modal shape function of the beam section can be expressed as

$$\begin{aligned} \Theta(x) &= A\text{acos}(\alpha x) - Ab\sin(\alpha x) + B\text{cch}(\beta x) + Bd\text{sh}(\beta x), \\ A &= \left(1 + \frac{\rho h^2 p^2}{\mu G}\right)\alpha - \frac{EI}{\mu AG}\alpha^3, \\ B &= \left(1 + \frac{\rho h^2 p^2}{\mu G}\right)\beta + \frac{EI}{\mu AG}\beta^3. \end{aligned} \quad \text{(B.15)}$$

According to $\gamma = \theta - \partial y/\partial x$, the shear angle modal shape function of the beam can be expressed as

$$\begin{aligned} \Gamma(x) = (A - \alpha)a\cos(\alpha x) - (A - \alpha)b\sin(\alpha x) \\ + (B - \beta)c\text{ch}(\beta x) + (B - \beta)d\text{sh}(\beta x). \end{aligned} \quad \text{(B.16)}$$

In the case of small rotation angle of the beam section, the bending moment modal shape function $\bar{M}(x)$ of the beam can be derived by Equation (B.15)

$$\begin{aligned} \bar{M}(x) = EI(-A\alpha a\sin(\alpha x) - A\alpha b\cos(\alpha x) \\ + B\beta\text{csh}(\beta x) + B\beta\text{dch}(\beta x)). \end{aligned} \quad \text{(B.17)}$$

Data Availability

Conflicts of Interest

The authors declare that there are no conflicts of interest regarding the publication of this paper.

Acknowledgments

This article is at the authors' own expense.

References

[1] J. T. Shang, X. Chu, and D. He, "Preparation of three-dimensional shaped aluminum alloy foam by two-step foaming," *Materials Science and Engineering: B*, vol. 151, no. 2, pp. 157–162, 2008.

[2] E. Guglielmino, G. Epasto, and V. Crupi, "Impact response of aluminum foam sandwiches for light-weight ship structures," *Metals*, vol. 1, no. 1, pp. 98–112, 2011.

[3] H. Zhiwei, Z. Xinlei, L. Chun, and D. Qinwei, "Effects on the various aluminum foam fenders of a tripod offshore wind turbine collision due to a ship," *Marine Technology Society Journal*, vol. 54, no. 1, pp. 79–96, 2020.

[4] H. J. Luo, H. Lin, Z. H. Zhao, Y. H. Liu, and G. C. Yao, "Preparation of aluminum foam sandwich reinforced by steel sheets," *Procedia Materials Science*, vol. 4, no. 589, pp. 39–43, 2014.

[5] C. C. Ma and F. C. Lan, "Review the research trends and application in car body of aluminum foam," *Applied Mechanics and Materials*, vol. 729, pp. 73–78, 2015.

[6] F. Shadan, F. Khoshnoudian, and A. E. Andiari, "Structural damage identification based on strain frequency response functions," *International Journal of Structural Stability and Dynamics*, vol. 18, no. 12, article 1850159, 2018.

[7] D. H. Nguyen, L. V. Ho, T. Bui-Tien, G. D. Roeck, and M. A. Wahab, "Damage evaluation of free-free beam based on vibration testing," *Applied Mechanics*, vol. 1, no. 2, pp. 142–152, 2020.

[8] A. Esfandiari, M.-. S. Nabiyan, and F. R. Rofooei, "Structural damage detection using principal component analysis of frequency response function data," *Structural Control and Health Monitoring*, vol. 27, no. 7, 2020.

[9] H. Sahar and S. Fariba, "Using incomplete FRF measurements for damage detection of structures with closely-spaced eigenvalues," *Measurement*, vol. 188, no. 12, article 110388, 2022.

[10] W. Lestari, P. Qiao, and S. Hanagud, "Curvature mode shape-based damage assessment of carbon/epoxy composite beams," *Journal of Intelligent Material Systems and Structures*, vol. 18, no. 3, pp. 189–208, 2007.

[11] M. Cao, Y. Lin, and L. Zhou, "Sensitivity of fundamental mode shape and static deflection for damage identification in cantilever beams," *Mechanical Systems and Signal Processing*, vol. 25, no. 2, pp. 630–643, 2011.

[12] A. Saeed, W. Aashir, and S. V. Umar, "Multiple damage detections in plate-like structures using curvature mode shapes and gapped smoothing method," *Advances in Mechanical Engineering*, vol. 11, no. 5, Article ID 1687814019848921, 2019.

[13] C. Zhu, J. Wang, Z. Chen, and B. Liu, "Dynamic characteristic parameters identification analysis of a parallel manipulator with flexible links," *Journal of Mechanical Science and Technology*, vol. 28, no. 12, pp. 4833–4840, 2014.

[14] E. Reynders, G. Wursten, and G. de Roeck, "Output-only structural health monitoring in changing environmental conditions by means of nonlinear system identification," *Structural Health Monitoring*, vol. 13, no. 1, pp. 82–93, 2014.

[15] Y. F. Shi, Z. Li, and C. C. Chang, "Output-only subspace identification of structural properties and unknown ground excitation for shear-beam buildings," *Advances in Mechanical Engineering*, vol. 8, no. 11, Article ID 168781401667990, 2016.

[16] S. Amirali, M. Shapour, and S. K. Heidari, "Detectability conditions for output-only subspace identification," *Mathematical*

and Computer Modelling of Dynamical Systems, vol. 26, no. 1, pp. 55–79, 2020.

[17] H. S. Zhao, Y. F. Gao, and H. H. Liu, "Fault diagnosis of wind turbine bearing based on stochastic subspace identification and multi-kernel support vector machine," *Journal of Modern Power Systems and Clean Energy*, vol. 7, no. 2, pp. 350–356, 2019.

[18] X. Y. Li, Y. H. Guan, M. T. Luo, and B. Y. Wu, "Modal parameter identification of covariance-based stochastic subspace identification based on Welch method," *Chinese Journal of Theoretical and Applied Mechanics*, vol. 54, no. 10, pp. 2850–2860, 2022.

[19] B. Lukas, W. Marcel, and K. Peter, "Automated set-up parameter estimation and result evaluation for SSI-Cov-OMA," *Vibroengineering Procedia*, vol. 34, pp. 43–49, 2020.

[20] W. X. Ren, Y. Q. Lin, and S. E. Fang, "Structural damage detection based on stochastic subspace identification and statistical pattern recognition: I. Theory," *Smart Materials & Structures*, vol. 20, no. 11, article 115009, 2011.

[21] A. Cancelli, S. Laflamme, A. Alipour, S. Sritharan, and F. Ubertini, "Vibration-based damage localization and quantification in a pretensioned concrete girder using stochastic subspace identification and particle swarm model updating," *Structural Health Monitoring*, vol. 19, no. 2, pp. 587–605, 2020.

[22] M. Alexander, D. Michael, and C. E. Ventura, "A reliability-based approach to determine the minimum detectable damage for statistical damage detection," *Mechanical Systems and Signal Processing*, vol. 154, no. 1, 2021.

[23] C. Wang, M. H. Hu, Z. N. Jiang, Y. Zuo, and Z. Zhu, "A modal parameter identification method based on improved covariance-driven stochastic subspace identification," *Journal of Engineering for Gas Turbines and Power*, vol. 142, no. 6, pp. 061005–061019, 2020.

[24] L. J. Gibson and M. F. Ashby, *Cellular Solids: Preface to the second edition*, Cambridge University Press, 1997.

[25] H. P. Wang, P. Xiang, and X. Li, "Theoretical analysis on strain transfer error of FBG sensors attached on steel structures subjected to fatigue load," *Strain*, vol. 52, no. 6, pp. 522–530, 2016.

[26] H. Liu, Z. W. Zhu, Y. Zheng, B. Liu, and F. Xiao, "Experimental study on an FBG strain sensor," *Optical Fiber Technology*, vol. 40, pp. 144–151, 2018.

[27] H. P. Wang, L. Z. Jiang, and P. Xiang, "Improving the durability of the optical fiber sensor based on strain transfer analysis," *Optical Fiber Technology*, vol. 42, pp. 97–104, 2018.

[28] A. Nayyar, U. Baneen, S. A. Z. Naqvi, and M. Ahsan, "Detection and localization of multiple small damages in beam," *Advances in Mechanical Engineering*, vol. 13, 14 pages, 2021.

[29] K. Peng, H. Guo, and X. Shang, "EEMD and multiscale PCA-based signal denoising method and its application to seismic P-phase arrival picking," *Sensors*, vol. 21, no. 16, p. 5271, 2021.

[30] P. Upadhay, S. K. Upadhyay, and K. K. Shukla, "Denoising 1D signal using wavelets," *International Journal of Intelligent Systems Technologies and Applications*, vol. 19, no. 6, pp. 517–525, 2020.

[31] D. Dalalah and D. B. Hani, "On the actual and observed process capability indices: a signal-to-noise ratio model," *Measurement*, vol. 81, pp. 241–250, 2016.